Electrochemical oxidation of oxalic acid and hydrazinium nitrate on platinum in nitric acid media

L.C. Rockombeny[a], J.P. Féraud[a], B. Queffelec[b], D. Ode[a], T. Tzedakis[c,*]

[a] Commissariat à l'Énergie Atomique/Marcoule, DTEC/SGCS/LGCI, BP 17171, 30207 Bagnols sur Cèze, France
[b] SIER, 16 Avenue du petit Lac, 95210 St. Gratien, France
[c] Laboratoire de Génie Chimique, UMR 5503 CNRS, Université Paul Sabatier, 118, route de Narbonne, 31062 Toulouse, France

A B S T R A C T

Several studies in the literature have investigated the electrochemical effects of oxalic acid and hydrazine on various materials in neutral (pH buffered to 7), basic or weakly acidic media (pH 6). The present work proposes electrochemical techniques that allow for the study of the electrochemical behavior, on a Pt electrode, of oxalic acid and hydrazinium nitrate to better understand their oxidation mechanisms in a nitric acid medium at a pH below 1; in addition, some experiments were carried out to define an electrochemical method that would allow for the simultaneous detection of these species when present within process effluent in very acidic solutions. Some physical data regarding oxalic acid and hydrazinium nitrate were also determined: anodic oxidation of hydrazinium nitrate and oxalic acid were observed at 0.2 V and 0.7 V (vs. Ag/AgCl), respectively. The diffusion coefficients of hydrazinium nitrate and oxalic acid were found to be 5.2×10^{-6} and 2.9×10^{-7} cm^2 s^{-1}, respectively. An experimental design approach demonstrated the influence of nitric acid concentrations on the diffusion coefficients of these species.

1. Introduction

Numerous papers have addressed the electrochemical behavior of oxalic acid and hydrazine [1–20], often with respect to biology. Oxalic acid and hydrazine are detected by electrochemical methods in aqueous solution for pH levels ranging from 6 to 7.

Works on the oxidation of oxalic acid have focused on designing an oxalate-specific sensor; they have studied the mechanism of degradation during anodic oxidation. Cyclic or linear voltammetry [1,2,4–7,9–11] and chronoamperometry [3–5,8] are the main electrochemical techniques that have been used. Various massive materials (Pt [1], glassy carbon [1,4], etc.) and modified metals (dimensionally stable anodes, DSA, Ti coated by Pt or IrO_2 or RuO_2 [1], boron-doped diamond [7], etc.) are used as anodes. Graphite modified by palladium nanoparticles [4,6] and rhodium [8,11] have also been examined as catalysts for the electrochemical oxidation of oxalic acid. The results show that the oxidation potential of oxalic acid is influenced by the type of electrode used as well as its surface and composition. Adsorption (especially on Pt), passivation and interaction phenomena can influence the rate of this reaction.

Cyclic voltammetry [12–18], amperometric detection and/or differential pulse voltammetry [12] have been used to study the oxidation of hydrazine on modified glassy carbon electrodes [12–16]. Zinc oxide [17] and carbon nanotubes [18] have also been used for the development of a hydrazine electrochemical sensor. As for oxalic acid, the oxidation of hydrazine may be influenced by the type of electrode used as well as its surface state and composition and solution pH.

A bibliographical review has revealed no studies investigating the development of a method for detecting both oxalic acid and hydrazine present in the same medium.

The purpose of the present work was to carry out voltammetric measurements on oxalic acid and hydrazinium nitrate on a platinum electrode in a concentrated nitric acid medium to obtain a better understanding of their oxidation mechanisms and to develop an electrochemical method for their simultaneous detection when present within process effluent in very acidic solutions. Some physical data regarding oxalic acid and hydrazinium nitrate were also obtained.

2. Experimental procedures

The chemicals used were of analytical grade (purity >98.5%). Solid oxalic acid was provided by Sigma Aldrich (CAS: 61353566). Nitric acid possessed a density $\rho = 1.42$ g cm^{-3} (purity 65%). Hydrazinium nitrate was a laboratory-prepared solution. Concentrated nitric acid was added to hydrazine hydrate (CAS: 78035378) until complete neutralization at pH 4.5, forming hydrazinium

* Corresponding author. Tel.: +33 5 61 55 83 02; fax: +33 5 61 55 61 39.
E-mail address: tzedakis@chimie.ups-tlse.fr (T. Tzedakis).

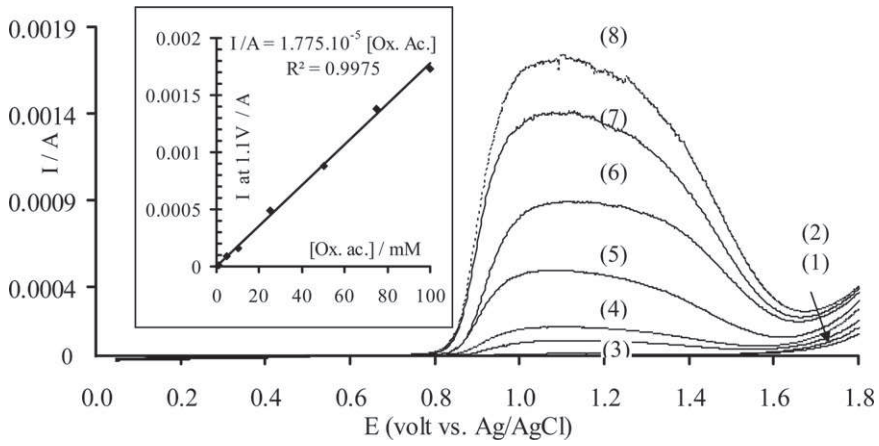

Fig. 1. [Ox. ac.] or oxalic acid's concentration dependence on the current–potential curves, obtained on Pt rotating disk. $\omega = 1000$ RPM: supporting electrolyte 2 M HNO_3; (1) no oxalic acid; (2) 1 mM; (3) 5 mM; (4) 10 mM; (5) 25 mM; (6) 50 mM; (7) 75 mM; (8) 100 mM; potential scan rate: 0.005 V s^{-1}. Inset: the variation of anodic current at 1.1 V vs. the oxalic acid concentration.

nitrate; this reaction is highly exothermic and can be explosive. Particular caution is required when using hydrazine hydrate because it is a CMR (carcinogenic, mutagenic and reprotoxic) substance.

All electrochemical measurements were carried out using an Autolab PGSTAT 30 potentiostat/galvanostat controlled with GPES 4.9 software and a three-electrode setup with a saturated silver reference electrode (Ag/AgCl, 3 M KCl), a platinum wire counter-electrode and a platinum-disk working electrode.

3. Results and discussion

3.1. Electrochemical kinetics on Pt rotating disk electrode

3.1.1. Oxalic acid

Linear voltammograms, obtained at the steady state (5 mV s^{-1}) with a Pt rotating-disk electrode ($\omega = 1000$ RPM) and various concentrations of oxalic acid in 2 M HNO_3, are shown in Fig. 1. A signal indicating the oxidation of oxalic acid to carbon dioxide on Pt according to equation (3.1.1.1) was observed for potentials higher than 0.7 V; simultaneously, bubbles appeared at the electrode surface. For low concentrations (curves (1)–(3)), the obtained signal shows a practically constant 'limiting current', with a slight decrease for potentials higher than 1.4 V. For concentrations above 10 mM, a peak-shaped curve was obtained and the magnitude of the current decreased nearly to zero for potentials higher than ~1.2 V; partial and reversible passivation of the platinum electrode caused by the gaseous carbon dioxide produced on the electrode surface could explain this decrease. Indeed, all of the curves obtained can be reproduced without mechanical treatment. The oxidation reaction can be written as follows:

$$HCOO{-}COOH \rightarrow 2CO_2 + 2H^+ + 2e^- \qquad (3.1.1.1)$$

A linear dependence of the anodic current (I_{max} recorded at 1.1 V) vs. the oxalic acid concentration observed in the range 1–100 mM (inset, Fig. 1) reflects a mass-transfer limitation, even if the magnitude of the current decreases for higher potentials:

$$I_{max\ \ at\ \ 1.1\,V(A)} = 1.77 \times 10^{-5}[\text{Ox. Ac.}]_{(\text{mmol L}^{-1})},$$

where $R^2 = 0.9975$.

Tafel plots ($\ln i = \ln i_0 + \alpha n F\eta/RT$) for curves obtained in 1 mM oxalic acid were used to determine the exchange-current density i_0, the electron-transfer coefficient α and the intrinsic heterogeneous electron-transfer coefficient k^0 (cm s^{-1}). The exchange-current density ($i_0 = nFk^0C^0$) was found to be 2×10^{-7} A cm^2. Assuming $n = 2$, α and k^0 were found to be 0.3 and 10^{-6} cm s^{-1}, respectively. The value of k^0 indicates that oxalic acid can be considered an irreversible system.

3.1.2. Hydrazinium nitrate

Linear voltammograms obtained at the steady state with a Pt rotating-disk electrode and various concentrations of hydrazinium nitrate in 2 M HNO_3 are shown in Fig. 2(a).

Considering that the final oxidation product is N_2, the overall oxidation reaction of hydrazinium nitrate can be written as follows:

$$N_2H_5^+ \rightarrow N_2 + 5H^+ + 4e^- \qquad (3.1.2.1)$$

The following results were obtained:

- For hydrazinium nitrate concentrations lower than 10 mM, classically shape curves were obtained, containing one wave beginning at ~0.2–0.4 V. The wave "plateau" with a limiting current clearly indicates a mass-transfer limitation (diffusion limitation). The magnitude of its limiting current increases linearly with the hydrazinium nitrate concentrations according to the relationship (3.1.2.2).

$$I/A = 7.37 \times 10^{-5} \cdot [\text{H}\ \ \text{Nitrate}] \quad R^2 = 0.9991 \qquad (3.1.2.2)$$

- For higher concentrations of hydrazinium nitrate (50–75 mM), the curves indicate three important modifications:
  - The beginning of the I/E curve for hydrazinium nitrate oxidation shifts to lower potentials when the concentration increases, meaning that the corresponding electroactive species is oxidized more easily.
  - Increasing the hydrazinium nitrate concentration causes two signals to appear, at 0.2–0.6 V and 0.7–1.2 V.
  - After the potential of the second signal was reached, the magnitude of the current decrease indicates the passivation of the platinum electrode. Nevertheless, the curves obtained can be reproduced without mechanical treatment, which suggests that this passivation is reversible. The final oxidation product of hydrazinium nitrate is gaseous nitrogen and the presence of a gaseous layer at the interface could explain the decrease in the magnitude of the current.

Two possible explanations could justify this behavior:

Assuming that one electron was exchanged through an elementary step, for hydrazinium nitrate oxidation, the global reaction

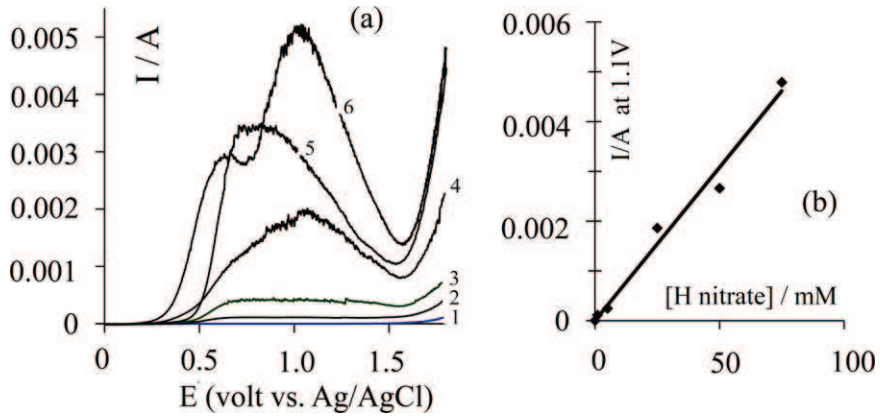

Fig. 2. (a) Hydrazinium nitrate's concentration dependence on the current–potential curves obtained on Pt rotating disk; $\omega = 1000$ RPM: supporting electrolyte 2 M HNO_3; (1) no hydrazinium nitrate; (2) 1 mM; (3) 5 mM; (4) 10 mM; (5) 25 mM; (6) 50 mM; (7) 75 mM; potential scan rate: 0.005 V s^{-1}. (b) Hydrazinium nitrate concentration dependence of the maximum anodic current (1.1 V).

(3.1.2.1) can be decomposed according to the following simplified scheme:

$$H_2N{-}NH_3^+ \rightarrow H_2N{-}NH_2^+ + e^- + H^+ \quad (3.1.2.1.a)$$

$$H_2N{-}NH_2^+ \rightarrow HN{=}NH_2^+ + e^- + H^+ \quad (3.1.2.1.b)$$

$$HN{=}NH_2^+ \leftrightarrow HN{=}NH + H^+ \quad (3.1.2.1.c)$$

$$HN{=}NH \rightarrow HN{=}NH^+ + e^- \quad (3.1.2.1.d)$$

$$HN{=}NH^+ \rightarrow N_2 + e^- + 2H^+ \quad (3.1.2.1.e)$$

(1) For hydrazinium nitrate concentrations lower than 10 mM, the curves show only one wave; thus, we can assume that the first electronic exchange ((3.1.2.1.a) and/or (3.1.2.1.b)) was the limiting step; this may correspond to 1 or 2 electrons exchanged and under these conditions, the exchange of the remaining electrons to obtain N_2 ((3.1.2.1.b) or (3.1.2.1.c) to (3.1.2.1.d)) occurs, during 'faster' steps.

When the hydrazinium nitrate concentration increases, high current values led to higher intermediate ($HN{-}NH_2^+$) concentrations. In addition, high H^+ concentrations, could be disadvantageous for the equilibrium (3.1.2.1.c), which may then cause the intermediate ($HN{-}NH_2^+$) to accumulate. Under these conditions, the oxidation of these intermediates ($HN{-}NH_2^+$) to nitrogen may occur at higher potentials (0.7–1.2 V) and lead to the second signal.

(2) Moisy et al. [21] presented the following chemical equilibrium between HNO_3 and hydrazinium nitrate for strongly acidic media:

$$N_2H_5^+ + HNO_3 \leftrightarrow N_2H_6^{2+} + NO_3^- \quad (3.1.2.3)$$

For hydrazinium nitrate concentrations lower than 10 mM, the solution contains mainly $N_2H_5^+$; thus, the curves show only one wave indicating the oxidation to nitrogen according to the previous statements. When the hydrazinium nitrate concentration increases, the equilibrium (3.1.2.3) shifts to the right and $N_2H_6^{2+}$ appears; its oxidation at more anodic potentials (0.7–1.2 V) can be observed separately from the wave of $N_2H_5^+$ oxidation.

Nevertheless, considering either explanation ((1) or (2)), the dependence of the maximum current (at 1.1 V) on the hydrazinium nitrate concentration for concentrations higher than 10 mM (Fig. 2b) seems to be quasi-linear in spite of a certain dispersion of the points.

$$I_{\text{current at 1.1 V A}} = -6.13 \times 10^{-5}[\text{H Nitrate}]_{\text{mmol L}^{-1}}, \quad R^2 = 0.979 \quad (3.1.2.4)$$

This linear evolution appears to be 'normal' because the final product (N_2) and, consequently, the overall electron number ($4e^-$) are the same. In addition, according to either the first or second explanation, the overall concentration of hydrazinium nitrate remains the same; therefore, the overall current (at 1.1 V) changes linearly with the concentration, in spite of the partial passivation of the electrode.

Tafel plots ($\ln i = \ln i_0 + \alpha nF\eta/RT$) for the curves obtained in 1 mM hydrazinium nitrate were also used to determine i_0, α and k^0. i_0 was found to be 4.4×10^{-5} A cm^2, assuming $n = 2$; α and k^0 were found to be 0.2 and 10^{-4} cm s^{-1}, respectively. This value of k^0 indicates the slightly irreversible electrochemical behavior of the hydrazinium nitrate/nitrogen system.

3.2. Electrochemical characterization of the systems by transient-state cyclic voltammetry and steady-state linear voltammetry

3.2.1. Oxalic acid

To obtain a better understanding of the oxalic acid oxidation mechanism, various cyclic voltammograms were recorded without stirring at different potential scan rates. The Pt-disk anode was immersed in a 5 mM solution of oxalic acid containing 2 M nitric acid. The analysis of the voltammograms (Fig. 3(a)) shows that the magnitude of the net current of the anodic peak observed at ~1 V increases linearly with the square root of the potential scan rate (Fig. 3(b)). This finding indicates that oxidation on Pt is not limited by adsorption phenomena [1] but rather is diffusion limited. On the other hand, the anodic curve contains only one signal, indicating that the two electrons are exchanged simultaneously. The cathodic peaks at $E = 0.4$ V were also obtained during the study of the supporting electrolyte and are not due to the oxalic acid/carbon dioxide system.

The representation of the potential of the anodic peak (E_{peak}) vs. the logarithm of the potential scan rate is indicative of the reversibility of the system [22]. For a simple electrochemical system, E_{peak} varies linearly with $\ln r$ in accordance with

$$E_{peak} = E^0 - \frac{R \times T}{\alpha \times n_\alpha \times F}\left[0.78 + \ln\frac{D^{0.5}}{k^0} + \ln\frac{\alpha \times n_\alpha \times F \times r^{0.5}}{R \times T}\right] \quad (3.2.1.1)$$

where E^0 is the standard potential of the electroactive system (V), n_α is the number of electrons exchanged in the charge-transfer step, k^0 is the intrinsic heterogeneous electronic transfer rate constant (cm s^{-1}), R is the gas constant (8.31 J mol^{-1} K^{-1}), T is the absolute temperature (K) and F is the Faraday constant (96,500 C mol^{-1}).

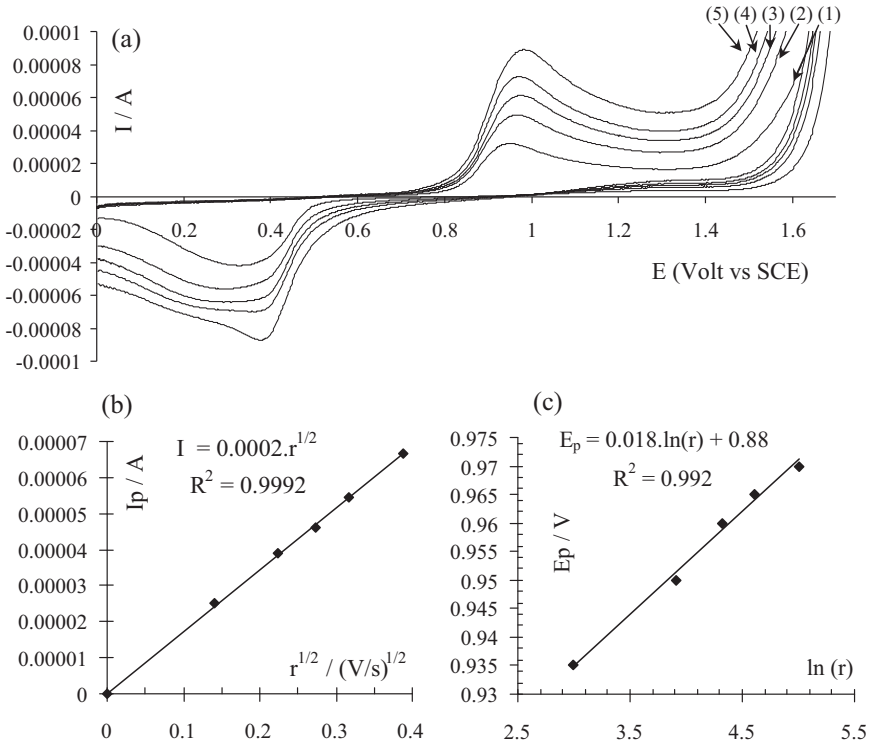

Fig. 3. (a) Potential scan rate dependence on the shape of cyclic voltammogramms obtained on a Pt rotating disk electrode ($S = 0.125\,cm^2$), immersed in 5 mM oxalic acid: supporting electrolyte 2 M HNO_3 without stirring; (1) $20\,mV\,s^{-1}$; (2) $50\,mV\,s^{-1}$; (3) $75\,mV\,s^{-1}$; (4) $100\,mV\,s^{-1}$; (5) $150\,mV\,s^{-1}$; (b) the anodic peak current I_{peak} vs. $r^{1/2}$ and (c) dependence of the peak potential E_{peak} vs. $\ln(r)$.

Fig. 3(c) shows the linear evolution of E_{peak} vs. $\ln r$ ($E_{peak(V)} = 0.881 + 0.018 \ln r_{(V\,s)}$ with $R^2 = 0.992$), indicating that the oxidation of oxalic acid to carbon dioxide is an irreversible process. The slope of this line, $(RT)/(2\alpha n_\alpha F) = 0.018$, indicates that $\alpha \times n_\alpha \approx 0.7$. Because two electrons are exchanged, $\alpha \approx 0.4$. On the other hand, the diffusivity of oxalic acid and the standard potential E^0 must be known to determine k^0 from the Y-intercept of this line:

$$0.881 = E^0 + \frac{R \times T}{\alpha \times n_\alpha \times F}\left[0.78 + \ln\frac{D^{0.5}}{k^0} + 0.5\ln\frac{\alpha \times n_\alpha \times F}{R \times T}\right].$$

In this study, the value 0.7 V vs. Ag/AgCl near $E_{I=0}$, in agreement with Fig. 4(a), was chosen as E^0 to estimate k^0. Under these conditions, the diffusion coefficient ($D_{\text{oxalic acid}}$) can be determined by the Levich equation (3.2.1.2):

$$I_{\text{lim},i} = 0.62 \times n \times S \times F \times D_i^{2/3} \times \omega^{1/2} \times \nu^{-1/6} \times C_i^{\text{sol}} \quad [22]\,(3.2.1.2)$$

where $I_{\text{lim},i}$ is the anodic limiting current, n is the overall number of electrons involved, C_i^{sol} is the concentration of species i in solution ($mol\,m^{-3}$), ω is the rotational speed of the electrode ($rad\,s^{-1}$), ν is the kinematic viscosity of the solution ($m^2\,s^{-1}$) and S is the geometric surface area of the working electrode (m^2) immersed in a 5 mM solution of oxalic acid. Several linear voltammograms were recorded at various angular velocities ω and the potential scan rate was $0.005\,V\,s^{-1}$ (Fig. 4(a)).

The increase in the anodic limiting current with ω reflects an increase in the flux of the electroactive species at the working electrode interface. The plot of the anodic limiting currents (I_{lim}) vs. the square root of the rotational speed ($\sqrt{\omega}$) in Fig. 4(b) shows a linear evolution and allows $D_{\text{oxalic acid}}$ to be determined. Using the Levich equation (3.2.1.2) and considering that $n = 2e^-$, $S = 0.03\,cm^2$ and $\nu = 10^{-2}\,cm^2\,s^{-1}$, $D_{\text{oxalic acid}}$ was found to be $2.9 \times 10^{-7}\,cm^2\,s^{-1}$. For comparison, chronoamperometry (Cottrell equation [22]) and/or voltammetry (Randles–Sevcik equation [22]) studies conducted at neutral pH [6,7,19] revealed values of $D_{\text{oxalic acid}}$ in the range 10^{-8} to $10^{-5}\,cm^2\,s^{-1}$. The wide dispersion of the $D_{\text{oxalic acid}}$ values is surprising and suggests possible interactions between oxalic acid molecules and/or between oxalic acid and nitric acid molecules.

Considering the diffusivity of oxalic acid ($2.9 \times 10^{-7}\,cm^2\,s^{-1}$) and the reported value of E^0 for oxalic acid, the intercept of the straight line (Fig. 3(c)) shows that $k^0 \approx 1.6 \times 10^{-6}\,cm\,s^{-1}$. This value is very sensitive because of the high uncertainty in the estimation of the intercept (Fig. 3(c)), but it verifies the value $10^{-6}\,cm\,s^{-1}$ obtained with Tafel's Law in Section 3.1.1. A study of the sensitivity of the oxalic acid diffusion coefficient depending on the operating conditions is detailed below.

3.2.2. Hydrazinium nitrate

Several cyclic voltammograms were recorded over a very wide range of potential scan rates ($20\,mV\,s^{-1}$ to $27.5\,V\,s^{-1}$) to better understand the mechanism of the anodic oxidation of hydrazinium nitrate. The potentiostat used was not compatible with potential scan rates higher than $27.5\,V\,s^{-1}$. The working electrode was immersed in a 5 mM solution of hydrazinium nitrate in 2 M nitric acid. The resulting cyclic voltammograms (Fig. 5) indicate an increase in the magnitude of the current of the oxidation peak observed at $E = 0.4$–0.5 V. The cathodic peak was also obtained during the study of the supporting electrolyte and thus was not due to the hydrazinium nitrate/nitrogen system. For potential scan rates higher than $3\,V\,s^{-1}$, a second signal appears at 0.8 V, indicating that the oxidation of hydrazinium nitrate on Pt involves at least two steps, with a relatively stable intermediate. A third oxidation shoulder appears at ~1.2 V when r exceeds $20\,V\,s^{-1}$. Hydrazinium nitrate is oxidized on Pt in two or three successive steps and tends to confirm the mechanism (3.1.2.1a)–(3.1.2.1e).

The magnitude of the oxidation peak current I_{peak} is plotted vs. $\sqrt{r}$ in Fig. 6(a). For potential scan rates ranging from 20 to $200\,mV\,s^{-1}$, I_{peak} increases linearly with $\sqrt{r}$, indicating that the

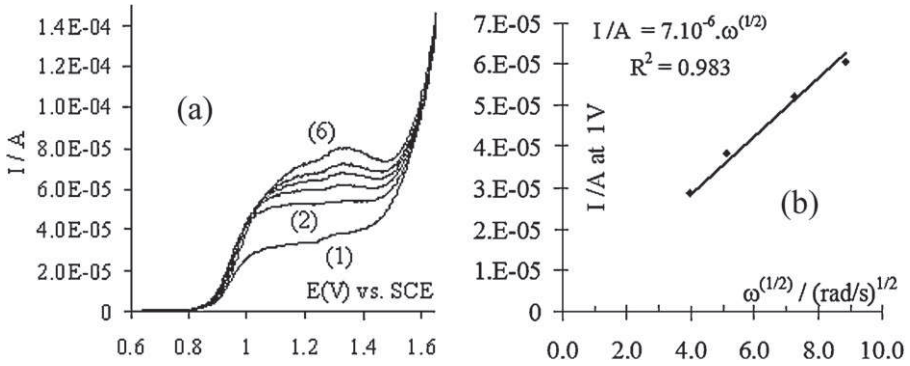

Fig. 4. (a) Influence of the angular velocity of the Pt rotating disk ($S = 0.125\ cm^2$) anode on the linear voltammogramms, obtained at the steady state (potential scan rate: $0.005\ V\ s^{-1}$). Oxalic acid 5 mM in 2 M HNO_3; (1) 250 rpm, (2) 500 rpm, (3) 750 rpm, (4) 1000 rpm, (5) 1250 rpm, (6) 2000 rpm; (b) the variation of anodic limiting currents vs. $\omega^{1/2}$.

oxidation of hydrazinium nitrate on Pt is limited by diffusion. For higher potential scan rates (in the range 0.2–27.5 $V\ s^{-1}$), the slope of the straight line decreases to the half of the previous value, indicating that mass transfer remains the limiting phenomenon. In addition, the number of exchanged electrons was divided by 2. A possible explanation could be that a first bi-electronic oxidation occurs for high values of r, followed by a second bi-electronic oxidation of the intermediate electrogenerated at the electrode.

Fig. 6(b) presents the evolution of the peak potential vs. the logarithm of the potential scan rate. Two different evolutions can be observed:

(i) For potential scan rates lower than $1\ V\ s^{-1}$, the increase of the peak potential vs. $\ln r$ was very slow ($E_{peak(V)} = 0.345 + 0.011\ \ln r_{(V\ s^{-1})}$; $R^2 = 0.81$), meaning that the corresponding electroactive system is practically reversible under the selected operating conditions. A similar treatment of oxalic acid (the diffusivity is discussed in next section) shows that $k^0 \approx 8 \times 10^{-3}\ cm\ s^{-1}$ and $\alpha \times n_\alpha \approx 1$. The value of k^0 confirms the slightly irreversible electrochemical nature of this system.

(ii) For potential scan rates higher than $1\ V\ s^{-1}$, Fig. 6(b) shows a linear evolution of the peak potential vs. $\ln r$ ($E_{peak(V)} = 0.22 + 0.0321\ \ln r_{(V\ s^{-1})}$; $R^2 = 0.94$). The ratio of the slopes for evolutions (i) and (ii) is equal to 3, which is related to a lower value of $\alpha \times n_\alpha$ for the corresponding electroactive system. Considering that only the first bi-electronic oxidation of hydrazinium nitrate was observed for high r values, the value of n_α in $\alpha \times n_\alpha$ could be lower and may provide a possible explanation for the observed results. On the other hand, operating at high potential scan rates leads to I/E curves being strongly

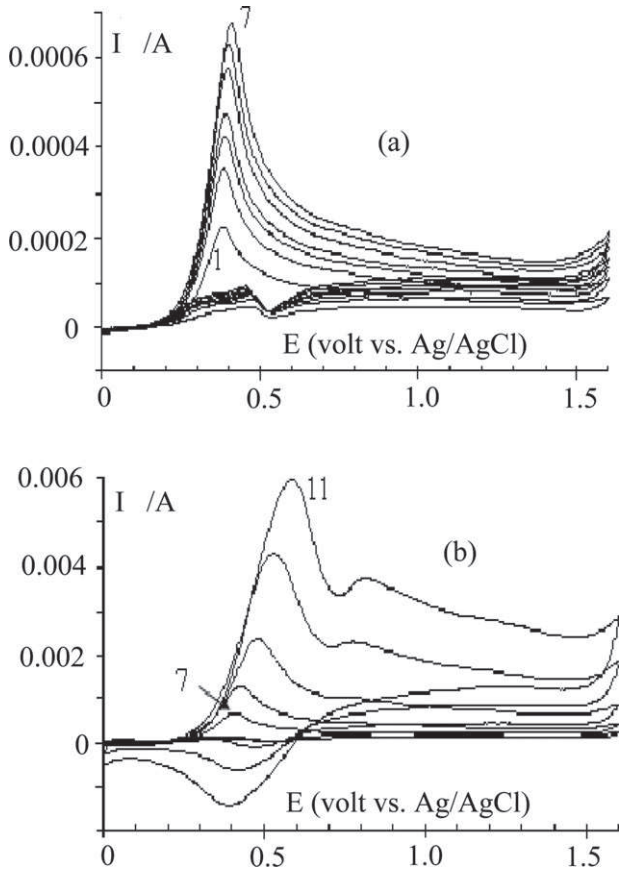

Fig. 5. Influence of the potential scan rate on the shape of cyclic voltammogramms obtained on Pt rotating disk, immersed in 5 mM hydrazinium nitrate in 2 M HNO_3; (a) (1) $20\ mV\ s^{-1}$; (2) $50\ mV\ s^{-1}$; (3) $75\ mV\ s^{-1}$; (4) $100\ mV\ s^{-1}$; (5) $150\ mV\ s^{-1}$; (6) $175\ mV\ s^{-1}$; (7) $200\ mV\ s^{-1}$; (b) (7) $200\ mV\ s^{-1}$; (8) $800\ mV\ s^{-1}$; (9) $3.2\ V\ s^{-1}$; (10) $12.8\ V\ s^{-1}$; (11) $27.5\ V\ s^{-1}$.

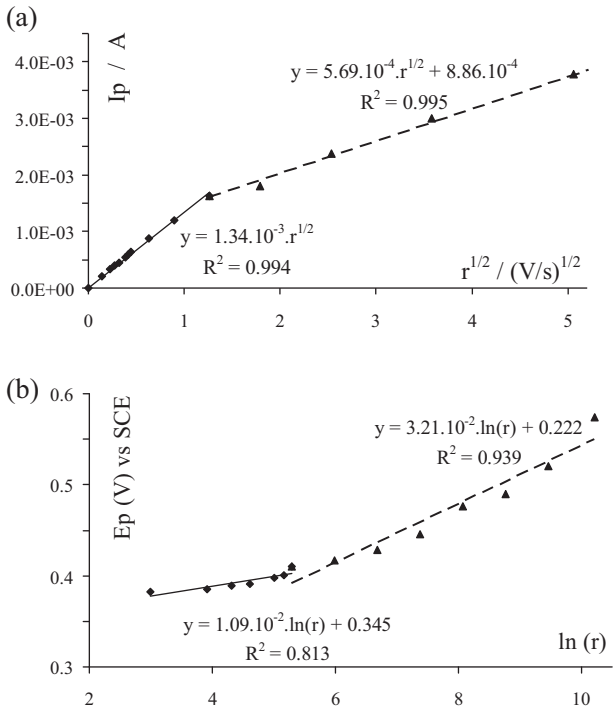

Fig. 6. (a) Evolution of the anodic peak current I_{peak} vs. $r^{1/2}$; (b) dependence of the peak potential E_{peak} vs. $\ln(r)$. Results of Fig. 5.

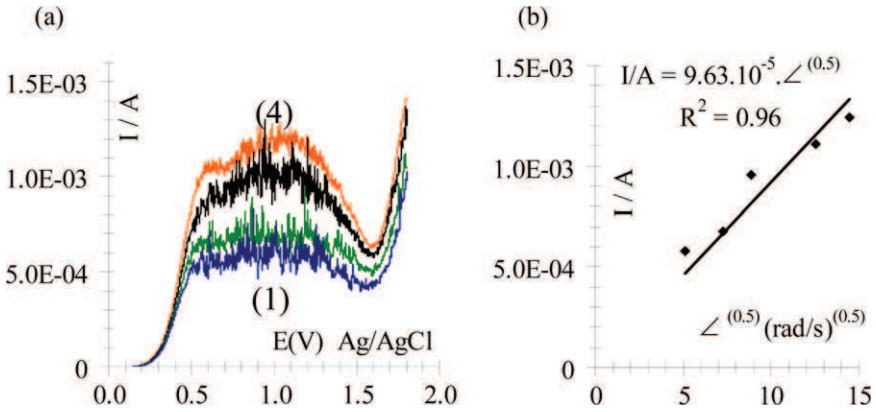

Fig. 7. (a) Influence of the angular velocity of the Pt rotating disk on the shape of current–potential curves, obtained with 5 mM hydrazinium nitrate in 2 M HNO_3. (1) 250 rpm; (2) 500 rpm; (3) 750 rpm; (4) 1500 rpm; (b) the variation of anodic maximum current (1–1.1 V) vs. $\omega^{0.5}$.

influenced by the ohmic drop caused by the solution between the working and reference electrodes. To obtain the true curves, the ohmic drop has to be compensated dynamically; unfortunately, the instruments that are available are unable to perform this operation.

To evaluate the diffusivity of hydrazinium nitrate, voltammograms were plotted at the steady state for various angular velocities of the Pt-disk anode (Fig. 7a); the working electrode was immersed in a 5 mM solution of hydrazinium nitrate and the potential scan rate was 0.005 V s^{-1}. Strong oscillations (noise) in the limiting part of the current potential curves were caused by nitrogen bubbles. For low angular velocities, the curves show one signal containing a diffusion wave at potentials ranging from 0.5 to 1.5 V. For angular velocities higher than 750 rpm, the curves clearly indicate a first signal (0.2–0.6 V) with a plateau at 0.55 V, followed by a second signal for potentials higher than 0.7 V. Even if the magnitude of this second signal decreases for potentials above 1.2 V, this drop does not irreversibly affect the electrode surface and these curves can be reproduced without any electrode treatment. A possible explanation for the current decrease could be the "masking" of the electrode by the large amount of nitrogen electrochemically generated at the anode.

The previously discussed acid–base equilibrium (cf (3.1.2.1)) allows various forms of hydrazinium nitrate to appear and could explain the presence of two very distinct signals. In addition, at high stirring rates, the high current amplitude resulted in large nitrogen bubbles, masking the disk surface. Intermediate forms of hydrazinium nitrate could then accumulate at the interface and their oxidation could be separately observed.

A linear evolution of the limiting current (at 0.7 V) vs. the square root of the angular velocity (Fig. 7(b)) was observed, meaning that the current was limited by mass-transfer phenomena. According to the Levich equation (3.2.1.2) and taking into account that $n = 4$, $S = 0.03\ cm^2$ and $\nu = 10^{-2}\ cm^2\ s^{-1}$, the value of $D_{hydrazinium\ nitrate}$ was found to be $5.2 \times 10^{-6}\ cm^2\ s^{-1}$. For comparison, studies of the oxidation of hydrazine in several media [12,15,18] reported values of $D_{hydrazine}$ ranging from 2.5×10^{-6} to $8.2 \times 10^{-6}\ cm^2\ s^{-1}$, similar to the value of $D_{hydrazinium\ nitrate}$ found in this work. However, hydrazinium nitrate exhibits complex chemistry in nitric acid media [21]; a study of the sensitivity of this diffusion coefficient depending on the operating conditions is detailed below.

3.3. Effects of the operating conditions on the diffusion coefficients

The previous experiments demonstrate the high sensitivity of the measurement of the diffusion coefficients due to the existence of molecular interactions and/or chemical equilibria, which may possibly be related to the activity of nitric acid. The approach detailed below was implemented to study this influence in an experimental design context. The methods used to analyze the results can be associated with a physical-response model based on experimental parameters with a minimum number of tests. Various experimental designs were implemented and analyzed with the software program Lumiere 4.45©.

3.3.1. Influence of oxalic acid and nitric acid concentrations on $D_{oxalic\ acid}$

In this study, given the number of factors (2) to be studied and assuming a linear experimental model, a 2^p full-factorial experimental design was used. The factors studied were the concentrations of oxalic acid and nitric acid; the response was $D_{oxalic\ acid}$ determined by chronoamperometry using the Cottrell equation with an applied potential of 1.1 V. The results are summarized in Table 1(a), where X_1 is the oxalic acid coded variable, X_2 is the nitric acid coded variable and K, the $D(X_1,X_2)$ ratio of $D(-1,-1)$, is a dimensionless response.

The analysis of this experimental design in coded variables and response K provided the correlation matrix (Table 1(b)). The diagonal of "1" shows that the main effects and second-order interactions do not overlap.

Table 1
(a) Effect of nitric acid on the diffusion coefficient of oxalic acid; (b) correlation matrix; (c) histogram of effects.

(a)

X_1	X_2	[Oxalic acid] (mM)	[Nitric acid] (M)	$D_{oxalic\ acid}$ ($cm^2\ s^{-1}$)	K
−1	−1	1	0.2	1.7E−08	1
1	−1	10	0.2	1.2E−08	0.71
−1	1	1	2	5.3E−07	31.1
1	1	10	2	4.3E−07	25.6

(b)

	X_1	X_2	$X_1 \times X_2$
X_1	1		
X_2	0	1	
$X_1 \times X_2$	0	0	1

(c)

Effects	%
X_2	97.99
X_1	1.11
$X_1 \times X_2$	0.9

The coefficients of the polynomial response vs. the main effects and interactions were calculated by multiple linear regression in the Lumiere program. Table 1(c) lists the coefficients according to their magnitude in the polynomial. This table shows the significant influence of the nitric acid concentration in the medium on $D_{\text{oxalic acid}}$. The plot of this polynomial response as a function of X_1 and X_2 indicates that the effect of the oxalic acid concentration on $D_{\text{oxalic acid}}$ is limited at low nitric acid concentrations (<1 M) but increases for higher nitric acid concentrations (≥1 M). This behavior may reflect the existence of interactions between oxalic acid molecules, for example the hydrogen bond [20], depending on the nitric acid conditions in the medium. A deviation of less than 15% between the mathematical model and the experimental result reflects the satisfactory agreement between the model and the experiment.

3.3.2. *Influence of the hydrazinium nitrate and nitric acid concentrations on $D_{\text{hydrazinium nitrate}}$*

Although $D_{\text{hydrazinium nitrate}}$ was consistent with the data reported in the literature, it seemed interesting with respect to the study of oxalic acid to determine the influence of two factors, the concentrations of hydrazinium nitrate and nitric acid, on the $D_{\text{hydrazinium nitrate}}$ response.

According to Moisy et al. and given the existence of two $N_2H_5^+/N_2H_6^{2+}$ chemical equilibrium constants (K_a = 0.09 [23] and K_a = 0.4 [24]) from 1 M in nitric acid, three full experimental designs were implemented in three levels. Thus, the peaks, the midpoint of each side and the center of a square define the experimental matrix.

The $D_{\text{hydrazinium nitrate}}$ response was determined by chronoamperometry with the Cottrell equation for an applied potential of 0.75 V. The results are summarized in Table 2(a)–(c), where X_1 is the hydrazinium nitrate coded variable, X_2 is the nitric acid coded variable and K, the $D(X_1;X_2)$ ratio of $D(-1,-1)$, is a dimensionless response. For Table 2(b) and (c), the hydrazinium nitrate concentrations were effective; therefore, the concentration of hydrazine introduced into the medium was determined from the different equilibrium constants such that the mean hydrazinium nitrate concentration was between 0.1 mM and 1 M.

The analysis of these experimental designs in coded variables and response K provided the correlation matrix (Table 2(d)). The diagonal of "1" shows that the main effects and second-order and quadratic interactions do not overlap.

The coefficients of each polynomial response as a function of the main effects and interactions were calculated by multiple linear regression in the Lumiere program. For each polynomial response, the values of these coefficients demonstrate the significant influence of the hydrazinium nitrate and nitric acid concentrations on $D_{\text{hydrazinium nitrate}}$. The plots of these polynomial responses as a function of X_1 and X_2 indicate the following:

- For low nitric acid concentrations (< 1 M), $D_{\text{hydrazinium nitrate}}$ decreases as the nitric acid concentration increases. In this case, it is possible to conclude that there is a good correlation between the mathematical model and the experiment; both revealed the existence of a maximum value for a hydrazinium nitrate concentration of 0.55 mM.
- For high nitric acid concentrations (≥1 M), when K_a = 0.09 [23], $D_{\text{hydrazinium nitrate}}$ again decreased as the HNO_3 concentration increased. However, above approximately 0.7 mM hydrazinium nitrate, $D_{\text{hydrazinium nitrate}}$ increased with the nitric acid concentration. In this case, the mathematical model was poorly correlated with the experimental values.
- For high nitric acid concentrations (≥1 M), when K_a = 0.4 [24], $D_{\text{hydrazinium nitrate}}$ again decreased as the HNO_3 concentration increased; however, above a nitric acid concentration of approximately 1.5 M, $D_{\text{hydrazinium nitrate}}$ increased with the nitric acid concentration. In this case, there was a good correlation between the mathematical model and the experimental values; both revealed the existence of a maximum value when the concentration of hydrazinium nitrate was 0.55 mM. These results confirmed that the value of K_a = 0.4 [24] closely approximates the $N_2H_5^+/N_2H_6^{2+}$ chemical equilibrium constant (3.1.2.2).

Table 2
Effect of nitric acid on the diffusion coefficient of hydrazinium nitrate: (a) with 0.2 ≤ [nitric acid] < 1 M; (b) with 1 ≤ [nitric acid] < 2 M and K_a = 0.09; (c) with 1 ≤ [nitric acid] < 2 M and K_a = 0.4; (d) correlation matrix.

(a)

X_1	X_2	[Hydrazinium nitrate] (mM)	[Nitric acid] (M)	$D_{\text{hydrazinium nitrate}}$ ($cm^2\ s^{-1}$)	K
−1	−1	0.1	0.2	6.2E−08	1
0	−1	0.55	0.2	5.7E−06	92
1	−1	1	0.2	2.3E−06	37
−1	0	0.1	0.6	5.2E−08	0.83
0	0	0.55	0.6	4.3E−06	70
1	0	1	0.6	1.9E−06	31
−1	1	0.1	1	5.6E−08	0.9
0	1	0.55	1	3.1E−06	50
1	1	1	1	2.3E−06	37
0	0	0.55	0.6	4.0E−06	65
0	0	0.55	0.6	4.4E−06	71
0	0	0.55	0.6	4.0E−06	65
0	0	0.55	0.6	4.5E−06	73

(b)

X_1	X_2	[Hydrazinium nitrate] (mM)	[Nitric acid] (M)	$D_{\text{hydrazinium nitrate}}$ ($cm^2\ s^{-1}$)	K
−1	−1	0.1	1	6.6E−05	1
0	−1	0.55	1	4.4E−06	0.06
1	−1	1	1	2.5E−06	0.04
−1	0	0.1	1.5	5.7E−05	0.9
0	0	0.55	1.5	3.3E−06	0.05
1	0	1	1.5	1.7E−06	0.02
−1	1	0.1	2	5.0E−05	0.8
0	1	0.55	2	3.8E−06	0.06
1	1	1	2	1.4E−06	0.02
0	0	0.55	1.5	3.0E−06	0.05
0	0	0.55	1.5	3.7E−06	0.06
0	0	0.55	1.5	3.4E−06	0.05
0	0	0.55	1.5	2.9E−06	0.04

(c)

X_1	X_2	[Hydrazinium nitrate] (mM)	[Nitric acid] (M)	$D_{\text{hydrazinium nitrate}}$ ($cm^2\ s^{-1}$)	K
−1	−1	0.1	1	1.7E−07	1
0	−1	0.55	1	2.9E−06	17
1	−1	1	1	8.0E−07	4.7
−1	0	0.1	1.5	8.7E−08	0.5
0	0	0.55	1.5	1.9E−06	11.2
1	0	1	1.5	1.0E−06	5.9
−1	1	0.1	2	1.1E−07	0.6
0	1	0.55	2	2.4E−06	14.1
1	1	1	2	8.0E−07	4.7
0	0	0.55	1.5	2.0E−06	11.8
0	0	0.55	1.5	1.8E−06	10.6
0	0	0.55	1.5	2.2E−06	12.9
0	0	0.55	1.5	1.9E−06	11.2

(d)

	X_1	X_2	$X_1 \times X_2$	X_1^2	X_2^2
X_1	1				
X_2	0	1			
$X_1 \times X_2$	0	0	1		
X_1^2	0	0	0	1	
X_2^2	0	0	0	0	1

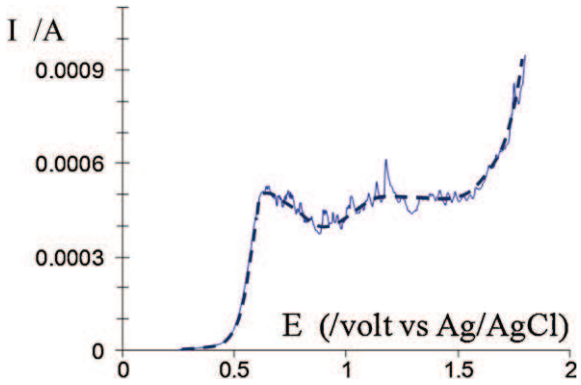

Fig. 8. Current potential curves obtained on the Pt rotating disk anode immersed within process effluent solution containing both hydrazinium nitrate and oxalic acid at 0.1 M in 2 M HNO_3. 1000 rpm; 25 °C; potential scan rate: 0.005 V s^{-1}.

3.4. Electrochemical behavior of both components in process effluent

Hydrazinium nitrate and oxalic acid were studied in process effluent in 0.1 M and 2 M nitric acid, respectively. As shown in Fig. 8, the two signals observed are attributed to hydrazinium nitrate and oxalic acid. The first signal, which is the hydrazinium nitrate signal, shows a maximum followed by a slight decrease in current caused by nitrogen bubbles. The second signal, which is attributed to the oxalic acid affected by nitrogen bubbles, is very noisy. Despites these noise problems, the results show that these species could be detected separately and in the case of their continuous and simultaneous detection, an optimized electrochemical cell must be designed to ensure the rapid and continuous removal of the electrogenerated bubbles and to improve the sensitivity of the electrochemical response of the system.

4. Conclusion

The oxidation of oxalic acid and hydrazinium nitrate was studied on a Pt anode in nitric acid media. The oxidation of oxalic acid was observed at 0.7 V (vs. Ag/AgCl) and carbon dioxide bubbles were observed on the surface of the electrode. Within an analytical framework, the influence of this phenomenon must be reduced because of the effect on the electroactive surface of the electrode. The electrokinetic parameters determined correspond to an irreversible system in which two electrons are exchanged simultaneously. In the oxalic acid concentration range from 1 mM to 100 mM, a linear evolution of the limiting current vs. the concentration was proposed.

The oxidation of hydrazinium nitrate begins at a potential of 0.3 V (vs. Ag/AgCl) and yields a separate signal from that of oxalic acid. The formation of nitrogen bubbles was observed for concentrations above 5 mM. Cyclic voltammetry studies were performed at high scan rates to try to understand the mechanism of hydrazinium nitrate electrooxidation. For high values of *r*, the results demonstrate that the oxidation of hydrazinium occurs in more than one step. A linear evolution of the limiting current vs. the concentration of hydrazinium nitrate was observed in the concentration range between 1 mM and 75 mM.

The diffusion coefficients of oxalic acid and hydrazinium nitrate in nitric acid media were determined; the values were 2.9×10^{-7} cm^2 s^{-1} and 5.2×10^{-6} cm^2 s^{-1}, respectively. As part of this determination, the experimental design approaches that were implemented revealed the influence of the nitrate concentration on these diffusion coefficients. For oxalic acid, this influence can be explained by the existence of hydrogen interactions between the molecules. For nitric acid concentrations higher than 1 M in nitric acid, hydrazinium nitrate forms divalent hydrazinium cations, whose presence strongly influences the value of the hydrazinium nitrate diffusion coefficient.

In acidic media, the two species can be detected at the same time, although bubbling effects interfere with the wave measurements. This work provides interesting perspectives with respect to the electrochemical analysis of these species, including the understanding of their oxidation processes.

References

[1] S. Ferro, C.A. Martinez-Huitle, A. De Battisti, Electro-oxidation of oxalic acid at different electrode materials, J. Appl. Electrochem. 40 (2010) 1779–1787.
[2] M.J. Chollier-Brym, F. Epron, E. Lamy-Pitara, J. Barbier, Catalytic and electrocatalytic oxidation of oxalic acid in aqueous solutions of different compositions, J. Electroanal. Chem. 474 (1999) 147–154.
[3] Chang-Zhi Zhao, Naoyoshi Egashira, Yoshiaki Kurauchi, Kazuya Ohga, Electrochemiluminescence oxalic acid sensor having a platinum electrode coated with chitosan modified with a ruthenium (II) complex, Electrochim. Acta 43 (1998) 2167–2173.
[4] Naoyoshi Egashira, Hirofumi Kumasako, Yoshiaki Kurauchi, Kazuya Ohga, Selective determination of oxalate with a ruthenium(II) complex/nafion-modified electrode combined with a carbon dioxide sensor, Anal. Sci. 10 (1994) 405–408.
[5] Innocenzo G. Casellaa, Carlo G. Zambonina, Fabrizio Prete, Liquid chromatography with electrocatalytic detection of oxalic acid by a palladium-based glassy carbon electrode, J. Chromatogr. A 833 (1999) 75–82.
[6] Biljana Šljukić, Ronan Baron, Richard G. Compton, Electrochemical determination of oxalate at pyrolytic graphite electrodes, Electroanalysis 9 (2007) 918–922.
[7] Florica Manea, Ciprian Radovan, Ioana Corb, Aniela Pop, Georgeta Burtica, Plamen Malchev, Stephen Picken, Joop Schoonman, Electrochemical oxidation and determination of oxalic acid at an exfoliated graphite–polystyrene composite electrode, Sensors 7 (2007) 615–627.
[8] Yang Liu, Jianshe Huang, Dawei Wang, Haoqing Hou, Tianyan You, Electrochemical determination of oxalic acid using palladium nanoparticle-loaded carbon nanofiber modified electrode, Anal. Methods 2 (2010) 855–859.
[9] T.A. Ivandini, T.N. Rao, Akira Fujishima, Yasuaki Einaga, Electrochemical oxidation of oxalic acid at highly boron-doped diamond electrodes, Anal. Chem. 78 (2006) 3467–3471.
[10] Shin-ichi Yamazaki, Naoko Fujiwara, Kazuaki Yasuda, A catalyst that uses a rhodium phthalocyanin for oxalic acid oxidation and its application to an oxalic acid sensor, Electrochim. Acta 55 (2010) 753–758.
[11] Shin-ichi Yamazaki, Yusuke Yamada, Naoko Fujiwara, Tsutomu Ioroi, Zyun Siroma, Hiroshi Senoh, Kazuaki Yasuda, Electrochemical oxidation of oxalic acid by Rh octaethylporphyrin adsorbed on carbon black at low overpotential, J. Electroanal. Chem. 602 (2007) 96–102.
[12] Jing Li, Xiangqin Lin, Electrocatalytic oxidation of hydrazine and hydroxylamine at gold nanoparticle – polypyrrole nanowire modified glassy carbon electrode, Sensors Actuat. 126 (2007) 527–535.
[13] Abdollah Salimi, Layla Miranzadeh, Rahman Hallaj, Amperometric and voltammetric detection of hydrazine using glassy carbon electrodes modified with carbon nanotubes and catechol derivatives, Talanta 75 (2008) 147–156.
[14] Yogeswaran Umasankar, Tzu-Yen Huang, Shen-Ming Chen, Vitamin B12 incorporated with multiwalled carbon nanotube composite film for the determination of hydrazine, Anal. Biochem. 408 (2011) 297–303.
[15] Hamid R. Zare, Navid Nasirizadeh, Hematoxylin multi-wall carbon nanotubes modified glassy carbon electrode for electrocatalytic oxidation of hydrazine, Electrochim. Acta 52 (2007) 4153–4160.
[16] Jyh-Myng Len, Jen-Sen Tang, Flow injection amperometric detection of hydrazine by electrocatalytic oxidation at a perfluorosulfonated lonomer/ruthenium oxide pyrochlore chemically modified electrode, Anal. Chem. 67 (1995) 208–211.
[17] Cuihong Zhang, Guangfeng Wang, Yulan Ji, Min Liua, Yuehua Feng, Zhidan Zhang, Bin Fang, Enhancement in analytical hydrazine based on gold nanoparticles deposited on ZnO–MWCNTs films, Sensors Actuat. B 150 (2010) 247–253.
[18] Yuan-Di Zhao, Wei-De Zhang, Hong Chen, Qing-Ming Luo, Anodic oxidation of hydrazine at carbon nanotube powder microelectrode and its detection, Talanta 58 (2002) 529–534.
[19] C. Bock, A. Smith, B. MacDougall, Anodic oxidation of oxalic acid using WOx based anodes, Electrochim. Acta 48 (2002) 57–67.
[20] Mariusz P. Mitoraj, Rafał Kurczab, Marek Boczar, Artur Michalak, Theoretical description of hydrogen bonding in oxalic acid dimer and trimer based on the combinedextended-transition-state energy decomposition analysis and

natural orbitals for chemical valence (ETS-NOCV), J. Mol. Model. 16 (2010) 1789–1795.
[21] A.C. Kappenstein, Ph. Moisy, G. Cote, P. Blanc, Contribution of the concept of simple solutions to calculation of the stoichiometric activity coefficients and density of ternary mixtures of hydroxylammonium or hydrazinium nitrate with nitric acid and water, Phys. Chem. Chem. Phys. 2 (2000) 2725–2730.
[22] A.J. Bard, L.R. Faulkner, Électrochimie: principes, méthodes et applications, Masson, Paris, 1983.
[23] W.E. Schimdt, Hydrazine and its Derivatives, Jonh Wiley and Sons, New York, 1984.
[24] S. Kotrly, L. Sucha, Handbook of Chemical Equilibria in Analytical Chemistry, Ellis Horwood, Chichester, 1985.